Theoretical Performance Analysis of Vehicular Broadcast Communications at Intersection and their Optimization

1st Tatsuaki Kimura
Graduate School of Engineering
Osaka University, Osaka, Japan
kimura@comm.eng.osaka-u.ac.jp

2nd Hiroshi Saito
Mathematics and Informatics Center
University of Tokyo, Tokyo, Japan
saito@mi.u-tokyo.ac.jp

***Abstract*—Cooperative vehicle safety (CVS) systems are a key application of intelligent transportation systems because they include many applications, such as cooperative collision warning. In CVS systems, vehicles periodically broadcast their information, e.g., position and speed. In this paper, we propose an optimization method for the broadcast rate in vehicle-to-vehicle (V2V) broadcast communications at an intersection on the basis of theoretical analysis. We consider a model in which locations of vehicles are modeled separately as *queuing* and *running* segments and derive key performance metrics of V2V broadcast communications via a stochastic geometry approach. Since these theoretical expressions are mathematically intractable, we develop *closed-form* approximate formulae for them. Using them, we optimize the broadcast rate such that the mean number of successful receivers per unit time is maximized. Because of the closed form approximation, the optimal rate can be used as a guideline for a *real-time* control-method. We evaluated our method through numerical examples and demonstrated the effectiveness of our method.**

***Index Terms*—ITS; V2V communication; stochastic geometry; broadcast; Poisson point process; intersection**

I. Introduction

Intelligent transportation systems (ITSs) are promising technology for improving safety for drivers/pedestrians and the efficiency of transportation [1]. In general, vehicle-to-infrastructure (V2I) and vehicle-to-vehicle (V2V) communications play a key role in achieving ITSs. These communications are commonly based on narrow-band dedicated short range protocols (DSRC). For instance, wireless access in vehicular environments (WAVE) is the protocol suite adopted in the U.S. In WAVE, IEEE 802.11p [2] is standardized for the media access control (MAC) and physical layers.

Cooperative vehicle safety (CVS) systems [3] are one of the key applications of ITSs using V2V communications. CVS systems include many applications such as cooperative collision warning and emergency brake lights [4]. In these systems, vehicles periodically broadcast their information e.g., positions (Global Positioning System; GPS), speed, and braking status, so that vehicles can track the positions of other vehicles and avoid traffic congestion, collisions, or unknown hazards. CVS systems have been attracting much attention in recent decades because these applications will drastically change our lives.

Because of the critical nature of CVS systems, their performance analysis and management are hot research topics. Broadcasting with a high transmission power and high broadcast rate in congested roadways may significantly degrade the wireless communication quality due to high interference. To reduce the interference caused by a large number of vehicles sharing the same channel, several schemes have recently been proposed to adaptively control the transmission power or broadcasting rate [4]–[9]. However, most of these schemes are not based on theoretical analysis and are commonly evaluated through simulations. Furthermore, most studies consider only *homogeneous* environments, such as multi-lane highways, in which vehicles are distributed with the same traffic density. However, to deploy CVS systems in urban environments, more realistic *inhomogeneous* situations, such as intersections, must be taken into account. More specifically, the density of vehicles near an intersection is much higher than that on a normal road due to queuing vehicles and crossing streets, and thus the interference near the intersection also becomes much higher.

In this paper, we propose an optimization method for V2V broadcast communications at an intersection on the basis of theoretical analysis. By deriving performance metrics of V2V broadcast communications and expressing them as tractable approximate formulae, we can optimize the broadcast rate in a reasonable computational time so that the number of successful receivers per unit time is maximized. We consider an intersection model, in which locations of vehicles are separated into *queuing* segments and *running* segments. In the former, vehicles are assumed to be queuing at even intervals; and in the latter, vehicles are distributed in accordance with a homogeneous Poisson point process (PPP). By using a stochastic geometry approach, theoretical values are derived for the two key performance metrics of V2V broadcast communications: the probability of successful transmission and the mean number of successful receivers. However, these results from exact analysis are expressed in *non-analytical* form and require time-consuming numerical computation. Thus, they are too complicated for not only the forms of the function to be understood but also their system parameters to be optimized. To address this problem, we developed a closed-

form approximation for the performance metrics by assuming sufficiently large queues. Using the approximate formulae, we optimize the broadcast rate of vehicles that maximizes the number of successful receivers per unit time. The closed-form expression enables us to easily compute the optimal broadcast rate without time-consuming numerical computation. Numerical results revealed the proposed optimization could mitigate the interference problem at an intersection. We also found that our approximation fitted well to both simulation and exact analysis.

II. Related work

To reduce the interference of V2V communications in CVS systems, several adaptive control schemes for transmission power [4], [8], [9] or broadcasting rate [4]–[7] have been proposed. For example, the method proposed by Torrent-Moreno et al. [8] adaptively controls the transmission power of vehicles so that their max-min fairness is satisfied. Huang et al. [4] developed broadcast rate and power control algorithms, in which the rate is determined by estimating the channel error rate and the power is determined by observing the channel status. Fallah et al. [6] updated a previous algorithm [5] so that the power changes in each iteration can be configurable and stable. The adaptive control methods above were not based on theoretical interference analysis and were considered in simple environments such as multi-lane highways. However, theoretical guidelines for more realistic situations, such as intersections, are crucial to deploy CVS systems in more complex urban environments.

Stochastic geometry is a powerful mathematical tool for modeling random spatial events and has been applied to the area of vehicular networks [10]–[18]. In previous studies [12], [13], the behavior of CSMA used in DSRC was analyzed. More specifically, Tong et al. [13] studied the performance of DSRC in both the spatial and time domains by using a Markov chain model approach for CSMA, which is similar to that of Nguyen et al. [14]. More recently, Chetlur and Dhillon [15] studied V2V communications where vehicles are distributed on roads that is randomly distributed according to Poisson line process. Similarly, by considering the spatial patterns of and vehicles on roads and cellular base stations together, Choi and Baccelli [16] analyzed the coverage probability of cellular-assisted vehicular communications. However, the above studies considered only homogeneous situations and did not consider power or broadcast rate control. Similar to us, Steinmetz et al. [17] analyzed packet reception probability at an intersection by modeling the locations of vehicles as a homogeneous PPP. They also considered an inhomogeneous PPP scenario as an extension, but no specific intensity function of vehicular density was given. In our previous study [18], we directly modeled the queueing segment in an intersection and proposed optimization of transmission power based on theoretical analysis. However, the obtained analytical results are highly complicated and mathematically intractable. Contrary to these studies, we propose a real-time broadcast rate optimization method by deriving tractable results.

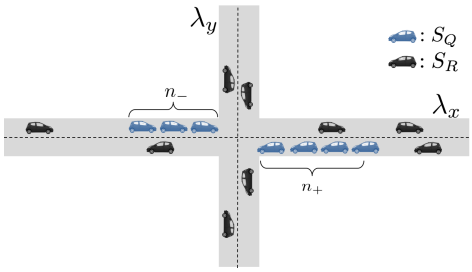

Fig. 1. System model. Vehicles in running segment (S_R) are distributed in accordance with homogeneous PPP with intensity λ_x or λ_y. n_+ and n_- represent number of vehicles stopping at intersection.

III. Model description

Figure 1 shows a conceptual image of our model. We consider an intersection where two streets are crossing. One street runs parallel along the x-axis, and the other along the y-axis. On the street along the x-axis, vehicles are queuing, i.e., stopped, at the intersection, and on both streets, vehicles are running. We call these parts a queuing segment S_Q or a running segment S_R. In addition, S_{R_x} and S_{R_y} denote the running segments on the x- or y-axis, respectively. We assume that vehicles in S_R are distributed in accordance with a homogeneous PPP on each street. Let λ_x and λ_y denote the intensity of vehicles in S_{R_x} and S_{R_y}. Let n_+ and n_- denote the numbers of vehicles stopped at an intersection in each part, where the subscript $\{+,-\}$ represents the positive or negative part on the x-axis. We assume that vehicles have length l_v and the widths of the streets (i.e., those of vehicles) are negligible. Note that there is no queue on the y-axis because we consider the case where the traffic signals on the y-axis are green. We can apply the same discussion in this paper to the case where those on the x-axis are green.

We next explain the channel model. Vehicles periodically broadcast a packet and each transmission requires L [sec.]. We assume that vehicles in S_Q independently transmit with rate $\theta \in (0, 1/L)$ [1/sec.] and those in S_R with $\theta_0 \in (0, 1/L)$. If time is slotted and each slot size is L, then each vehicle transmits at each time-slot in accordance with an independent Bernoulli distribution. More specifically, the probability (i.e., the parameter of Bernoulli distribution) that each vehicle in S_Q (resp. in S_R) is transmitting in each time slot is $\rho \triangleq \theta L \in (0, 1)$ [resp. $\rho_0 \triangleq \theta_0 L \in (0, 1)$]. Since θ and ρ (θ_0 and ρ_0) have one-to-one correspondence, we only consider ρ and ρ_0 hereafter. We also assume that vehicles currently transmitting cannot receive a packet from other vehicles at the same time. The transmission power of all vehicles is normalized to 1. In addition, all transmission channels have the effect of Rayleigh fading and h denotes the random variable that represents the fading gain. The path loss model is $r^{-\alpha}$ for distance $r \in \mathbb{R}_+$ and where $\alpha > 1$ is a path loss exponent. Thus, the received power from vehicle x_i at distance r can be expressed as $h_i r^{-\alpha}$.

Note that CSMA is designed as the MAC layer protocol in IEEE 802.11p [19]. However, models for CSMA networks are not mathematically tractable [13], [14], [20]. In addition,

Nguyen et al. [12] claimed that CSMA behaves like an ALOHA-type transmission pattern in dense networks. This is mainly because there are nodes that choose the same back-off counter due to finite collision window size in the binary exponential backoff of CSMA [12]. Indeed, Tong et al. [13] showed that results with an ALOHA-type model were similar to those obtained by NS2 simulation that models the CSMA behavior in their numerical examples. Therefore, we assume the ALOHA-type MAC protocol and model the locations of vehicles by a PPP. Note that in such a model, each vehicle attempts to transmit a packet with a certain probability in each time slot, and thus the positions of transmitters can be modeled by independent thinning of the original PPP (see e.g., [10]).

Let I denote the total received interference from all the vehicles. If we consider the tagged channel in which the communication distance is equal to r, the signal-to-interference-ratio (SIR) can be written as $\mathsf{SIR}_r = hr^{-\alpha}/I$. We then define the probability of successful transmission as the probability that the SIR of a tagged receiver exceeds a threshold T, i.e.,

$$p(r) \triangleq \mathsf{P}(\mathsf{SIR}_r > T) = \mathsf{P}\left(\frac{hr^{-\alpha}}{I} > T\right) \overset{(a)}{=} \mathbb{E}_I\left[\exp\left(-Tr^{\alpha}I\right)\right] = \mathcal{L}_I(Tr^{\alpha}), \quad (1)$$

where $\mathcal{L}_I(s)$ is the Laplace transform of I and (a) holds due to Rayleigh fading assumption.

A. Performance Metrics

In this section, we provide theoretical expressions of performance metrics of V2V communications.

1) Interference distributions: We first consider the interference from vehicles in S_Q. For this purpose, we assume that a tagged receiver is in the positive part on the x-axis and at distance d from the intersection. In addition, let $d_m = |d - ml_v|$ $(1 \le m \le n_- + n_+)$ denote the distance between the tagged receiver and the m-th vehicle from the intersection. Therefore, the total interference power received from S_Q is $I_Q \triangleq \sum_{m=1}^{n_-+n_+} h_m\delta_m d_m^{-\alpha}$, where $\delta_m = 1$ if the m-th vehicle transmits, and $\delta_m = 0$ otherwise. Recall that h_m is exponential with mean 1 (the Rayleigh fading assumption). Recall also that the vehicles in the S_Q are transmitting with the probability ρ. Therefore, the Laplace transform of I_Q, $\mathcal{L}_{I_Q}(s \mid d) \triangleq \mathbb{E}_{I_Q}[\exp(-sI_Q) \mid d]$, is equal to

$$\mathcal{L}_{I_Q}(s \mid d) = \mathbb{E}_{I_Q}\left[\exp\left(-s\sum_{m=1}^{n_-+n_+} h_m\delta_m d_m^{-\alpha}\right)\middle| d\right] = \prod_{m=1}^{n_-+n_+}\left[\frac{\rho}{1+\frac{s}{(d_m)^{\alpha}}} + 1 - \rho\right]. \quad (2)$$

We next consider the interference from the vehicles in S_R. Similar to the previous case, we assume that a tagged receiver is at distance d from the intersection in the positive part on the x-axis. Let Φ_R^X and Φ_R^Y denote PPPs corresponding to S_{R_x} and S_{R_y}. The total interference from Φ_R^X can be represented as $I_R^X = \sum_{x_i\in\Phi_R^X} h_i|x_i - d|^{-\alpha}$. Recall that vehicles in S_R transmit with probability ρ_0. By following a well-known computation of the Laplace functional of the Poisson point process (see e.g., Proposition 1.5 and Corollary 2.9 in [22]), we can compute the Laplace transform of I_R^X as follows.

$$\begin{aligned}\mathcal{L}_{I_R^X}(s) &\triangleq \mathbb{E}_{I_R^X}\left[\exp\left(-s\sum_{x_i\in\Phi_R^X}\frac{h_i\delta_i}{|x_i-d|^{\alpha}}\right)\right] \\ &= \exp\left(-\rho_0\lambda_x\int_{-\infty}^{\infty}\frac{s}{|x|^{\alpha}+s}\mathrm{d}x\right) \\ &= \exp\left(-\rho_0\lambda_x\frac{2\pi}{\alpha}\mathrm{cosec}\left(\frac{\pi}{\alpha}\right)\right). \end{aligned} \quad (3)$$

Note that the distance from the tagged transmitter to a vehicle at distance y from the intersection on the y-axis is equal to $\sqrt{y^2+d^2}$. Thus, if I_R^Y denotes the total interference from Φ_R^Y, we have $I_R^Y = \sum_{y_i\in\Phi_R^Y} h_i(y_i^2+d^2)^{-\alpha/2}$. Therefore, similar to (3), we obtain (see also Section 2 in [18]),

$$\begin{aligned}\mathcal{L}_{I_R^Y}(s \mid d) &\triangleq \mathbb{E}_{I_R^Y}\left[\exp\left(-s\sum_{y_i\in\Phi_R^Y}\frac{h_i\delta_i}{(y_i^2+d^2)^{\frac{\alpha}{2}}}\right)\middle| d\right] \\ &= \exp\left(-\rho_0\lambda_y\int_{-\infty}^{\infty}\frac{s}{(y^2+d^2)^{\frac{\alpha}{2}}+s}\mathrm{d}y\right). \end{aligned} \quad (4)$$

2) Probability of successful transmission: Note that the total interference from all the vehicles can be represented as $I = I_Q + I_R^X + I_R^Y$. Thus, by applying this to (1), we can easily obtain the probability of successful transmission as follows.

Proposition 1 *If a transmitter is at distance d from an intersection, the probability of successful transmission to a receiver at distance r from the transmitter on the x-axis is given by*

$$p(r) = \mathcal{L}_{I_Q}(Tr^{\alpha} \mid d')\mathcal{L}_{I_R^X}(Tr^{\alpha})\mathcal{L}_{I_R^Y}(Tr^{\alpha} \mid d'), \quad (5)$$

where $d' = d + r$ if the receiver is on the right-hand side of the transmitter, and $d' = |d - r|$ otherwise.

Although Proposition 1 only shows the case where a transmitter and receiver are on the x-axis, we can easily consider the case where they are on the y-axis.

3) Mean number of successful receivers: Using Proposition 1, we can also obtain the mean number of successful receivers, which is defined as the expected number of vehicles to which the tagged transmitter can transmit. The same metric is also considered by Nguyen et al. [12]. Recall that there are three types of receivers: vehicles in S_Q, in S_{R_x}, and in S_{R_y}. Recall also that vehicles transmitting radio waves cannot simultaneously receive information from other vehicles. As a result, we obtain the following result (for details, see [21]).

Proposition 2 *The mean number of successful receivers $\overline{M}$ for a transmitter at a distance $d > 0$ from an intersection is given by*

$$\overline{M} = (1-\rho)\sum_{i=-n_-}^{n_+} p(|d - il_v|) + (1-\rho_0) \times \left[\lambda_x\int_{\mathbb{R}} p(r)\mathrm{d}r + \lambda_y\int_{\mathbb{R}} p(\sqrt{d^2+r^2})\mathrm{d}r\right]. \quad (6)$$

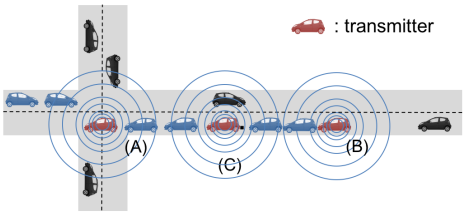

Fig. 2. Three typical cases considered in Section IV: target transmitter is (A) at intersection, (B) at end of queue, and (C) in middle of queue.

IV. Approximate Analysis

Although theoretical values of the performance metrics can be obtained as in Propositions 1 and 2, they are expressed in non-analytical forms (especially, due to the terms related to the interference from S_Q). Therefore, it is difficult not only to see the impacts of various parameters on them but also to optimize their system parameters because of time-consuming numerical computation. To solve this problem, we attempt to obtain a simple approximation for $p(r)$ and $\overline{M}$ that depends only on system parameters by assuming that the queue length is sufficiently large. We then optimize the broadcast rate of vehicles in S_Q (see Section V).

In general, the characteristics of $p(r)$ and $\overline{M}$ depend on the location of the tagged transmitter. To obtain approximation formulae, we consider three *typical* locations of the transmitter instead of considering arbitrary locations: the tagged transmitter is in the positive part on the x-axis and (A) at the intersection, (B) at the end of the queue, and (C) in the middle of the queue (see Figure 2). Since a vehicle at (or near) the intersection (case (A)) is affected by interferences from both parts (x- and y-axes) and queues, it is expected to have the worst performance. A vehicle near the end of the queue (case (B)) is said to be in an intermediate state of vehicles between the queuing and running segments. In case (C), if the queue is sufficiently long, the performance can be approximated as vehicles stopping at even intervals on a long 1-d line. As shown later, the performance of vehicles at other positions in the queue can be estimated by interpolating those in cases (A)–(C) (detailed discussion is in Section VI-C). In addition, we can estimate the other cases where the transmitter is in S_{R_x} or in S_{R_y} and far from the queue by ignoring the effect of the queue and considering vehicles homogeneously distributed on a 1-d line. Therefore, we analyze cases (A)–(C) because they characterize the effect of the intersection.

A. Case (A): Transmitter at Intersection

We start with case (A), where the transmitter is at an intersection. The main idea is the approximation of $\mathcal{L}_I(s \mid d)$ by considering a large queue. By expressing $\log \mathcal{L}_I(s \mid d)$ as an infinite series of the interference from each vehicle in the queue and considering a large queue, we can obtain a closed form approximation of $p(r)$. The detailed derivation is given in Appendix A and [21].

Approximate formulae of $p(r)$ in case (A): Suppose that the transmitter is at an intersection. If $(1-\rho)T \geq 1$[1] and $\alpha \in \mathbb{N}$, the probability of successful transmission can be approximated as follows: (i) If a receiver is the i-th vehicle from an intersection, then

$$p(il_v) \approx \frac{K(\rho)}{1-\rho} \exp\left[\left(2\xi_{\alpha,T}(\rho) - \rho_0\left(\lambda_x C^X_{\alpha,T} + \lambda_y C^Y_{\alpha,T}\right) l_v\right) i\right], \tag{7}$$

where

$$\xi_{\alpha,T}(\rho) = (\alpha + \kappa_{1,\alpha} - \kappa_{2,\alpha})((1-\rho)^{1/\alpha} - 1)T^{1/\alpha}, \tag{8}$$
$$\kappa_{1,\alpha} = \alpha \sum_{k=1}^{\infty} \frac{(-1)^{k+1}}{\alpha k - 1}, \quad \kappa_{2,\alpha} = \alpha \sum_{k=1}^{\infty} \frac{(-1)^{k+1}}{\alpha k + 1},$$

and

$$K(\rho) = \frac{1+T}{1+(1-\rho)T}, \tag{9}$$

$$C^X_{\alpha,T} = 2T^{\frac{1}{\alpha}} \frac{\pi}{\alpha} \mathrm{cosec}\left(\frac{\pi}{\alpha}\right), \quad C^Y_{\alpha,T} = \int_{\mathbb{R}} \frac{T \mathrm{d}y}{(y^2+1)^{\frac{\alpha}{2}} + T}, \tag{10}$$

(ii) if a receiver is in S_{R_x} at distance $r > 0$ from the intersection, then

$$p(r) \approx K(\rho) \exp\left[\left(\frac{2\xi_{\alpha,T}(\rho)}{l_v} - \rho_0\left(\lambda_x C^X_{\alpha,T} + \lambda_y C^Y_{\alpha,T}\right)\right) r\right], \tag{11}$$

and (iii) if a receiver is in S_{R_y} at distance $r > 0$ from the intersection, then

$$p(r) \approx \frac{K(\rho)}{(1-\rho)^{2r}} \exp\left[\left(-\frac{2\rho}{(\alpha+1)(1-\rho)Tl_v} + \frac{2\xi_{\alpha,T}(\rho)}{l_v} - \rho_0\left(\lambda_x C^X_{\alpha,T} + \lambda_y C^Y_{\alpha,T}\right)\right) r\right]. \tag{12}$$

Remark 1 If $\alpha = 2, 4$, $C^Y_{\alpha,T}$ can be computed as follows.

$$C^Y_{2,T} = \frac{T}{\sqrt{1+T}}, \qquad C^Y_{4,T} = \frac{\sqrt{T}\sqrt{\sqrt{1+T}-1}}{\sqrt{2}\sqrt{1+T}}.$$

Remark 2 The above approximate formulae (7), (11), and (12) suggest that, in our approximation, the probability of successful transmission decreases geometrically with the distance to receivers, and the decay rate is determined by only system parameters. In addition, if the parameters α and T that depend on a system or environment are given in advance, $\kappa_{1,\alpha}$, $\kappa_{2,\alpha}$, $C^X_{\alpha,T}$ and $C^Y_{\alpha,T}$ can be regarded as constant.

We next derive an approximate formula for the mean number of successful receivers using the previous results. Since the approximate formulae of $p(r)$ are expressed in a geometric form, we can also obtain a closed-form approximation for $\overline{M}$. Let $\overline{M}_Q(\rho)$, $\overline{M}_{R_X}(\rho)$, and $\overline{M}_{R_Y}(\rho)$ denote the mean numbers of successful receivers in S_Q, S_{R_x}, and S_{R_y}, respectively. First, applying (7) to Proposition 2 and considering sufficiently large n_+ and n_-, we obtain

$$\overline{M}_Q(\rho) \approx 2(1-\rho) \sum_{i=1}^{\infty} p(il_v).$$

[1] A typical value of the outage threshold T is 10–15 dB (for example, in IEEE 802.11p) In addition, the optimal ρ was less than 0.4 in our numerical examples. Thus, this assumption can be considered as valid.

Similar to the above, from (11) and (12), we can approximate $\overline{M}_{R_X}(\rho)$ and $\overline{M}_{R_Y}(\rho)$. Thus, under the same conditions as in $p(r)$, we obtain their approximation as follows.

Approximate formulae of $\overline{M}$ in case (A):

$$\overline{M}_Q(\rho) \approx \frac{2K(\rho)\exp\left(2\xi_{\alpha,T}(\rho) - \rho_0(\lambda_x C^X_{\alpha,T} + \lambda_y C^Y_{\alpha,T})l_v\right)}{1 - \exp\left(2\xi_{\alpha,T}(\rho) - \rho_0(\lambda_x C^X_{\alpha,T} + \lambda_y C^Y_{\alpha,T})l_v\right)}, \tag{13}$$

$$\overline{M}_{R_X}(\rho) \approx \frac{2K(\rho)(1-\rho_0)\lambda_x l_v}{2\xi_{\alpha,T}(\rho) - \rho_0(\lambda_x C^X_{\alpha,T} + \lambda_y C^Y_{\alpha,T})l_v}, \tag{14}$$

$$\overline{M}_{R_Y}(\rho) \approx 2(1-\rho_0)\lambda_y l_v K(\rho)\left[2\xi_{\alpha,T}(\rho) - 2\log(1-\rho) - \frac{2\rho}{(\alpha+1)(1-\rho)T} - \rho_0(\lambda_x C^X_{\alpha,T} + \lambda_y C^Y_{\alpha,T})l_v\right]^{-1}.$$

B. Case (B): Transmitter at End of Queue

We next consider case (B), where the tagged transmitter is at the end of the queue. In this case, the tagged transmitter is far from the y-axis due to the long queuing segment. Thus, we ignore the effect of interferes and receivers in the S_{R_y} because the vehicles that can successively receive a packet from the tagged transmitter are expected to be close to the transmitter. We divide this case into three sub-cases: a receiver is in (i) S_Q, in (ii) S_{R_x} in the negative part, or (iii) S_{R_x} in the positive part (see Figure 2). In addition, since the interference from the vehicles in S_{R_y} is assumed to be much smaller than that from S_Q and S_{R_x}, we ignore the term $\mathcal{L}_{I_Y}(Tr^\alpha \mid d)$, i.e., $p(r) \approx \mathcal{L}_{I_Q}(Tr^\alpha \mid d)\mathcal{L}_{I^R_X}(Tr^\alpha)$. Consequently, by applying a similar idea of the approximation in case (A), we obtain approximate formulae for $p(r)$ and $\overline{M}$ in this case. The expression of the formulae are given in Appendix B due to space limitation.

C. Case (C): Transmitter in Middle of Queue

Finally, we consider case (C), where the transmitter is in the middle of the queue. As well as case (B), if the queue is sufficiently long, then we can ignore the interferers and receivers in S_{R_y}. Thus, we approximate this case by considering vehicles queuing at even intervals on a single street with infinite length, i.e., a single infinite queue. Under this assumption, we can obtain approximate formulae for case (C) by simply removing the effect of the interference from vehicles on the y-axis in case (A). In other words, by substituting $\lambda_y = 0$ into (7), (11), (13), and (14), we can immediately obtain the results.

V. Broadcast Rate Optimization

We next consider the optimization of the broadcast rate of vehicles in the S_Q on the basis of the approximate formulae presented in Section IV. We assume that vehicles can determine their status (i.e., queuing or running) by tracking their speed. If the vehicles in S_Q transmit with a high broadcast rate, then they have higher interference than those in S_R due to the congestion of vehicles at the intersection. However, if a vehicle transmits with a high broadcast rate, it has more chance to successfully transmit to its neighbors (to be discovered by the neighbors). Thus, by carefully choosing the broadcast rate of the vehicles in S_Q, we can mitigate the interference and improve the performance of the V2V communication. To characterize and balance this relationship, we consider *the mean number of successful transmissions per unit time*, which is equal to

$$D(\rho) = \rho\overline{M}(\rho).$$

In the CVS systems, vehicles periodically transmit a packet so that other vehicles know their positions, i.e., they can be discovered by other vehicles. Therefore, this metric can be considered as the number of *discoveries* for a typical transmitter per unit time and a key performance metric in V2V broadcast communications. We can consider other metrics, such as probability of successful transmission to the nearest vehicle [18], however, to focus on the performance of the broadcast communication, we consider this metric. Using $D(\rho)$, we consider the optimization problem

$$\rho_* = \underset{0\le\rho\le 1}{\operatorname{argmax}}\ D(\rho).$$

By numerically solving the above problem, we can obtain the optimal broadcast rate that maximizes $D(\rho)$. Recall that the values from exact analysis shown in Propositions 1 and 2 require time-consuming numerical computation, and thus the optimization of $D(\rho)$ becomes much more time-consuming because of iterative computation in numerical optimization methods. However, by using the closed-form approximation of $D(\rho)$, we can compute the optimal ρ_* in a reasonable computational time. Indeed, if we assume that α, T, and ρ_0 are given in advance, ρ_* can be determined by only λ_x and λ_y. This fact suggests that if we prepare a look-up table in our vehicles that describes the optimal broadcast rate corresponding to each value of λ_x and λ_y, we can control the broad cast rate in (near-)optimal real-time manner.

Although $D(\rho)$ and the optimal ρ depends on the positions of the transmitters (i.e., cases (A)–(C)), we found that if the intensity in S_R is not very high, ρ_* is almost insensitive to the cases (A)–(C) in our numerical examples. Thus, we can obtain near-optimal broadcast rate regardless of the position of the tagged transmitter. We also found that they are mostly insensitive to n_+ and n_-, which indicates that our large queue assumption is valid for the broadcast rate optimization (see Section VI-B).

VI. Numerical Examples

In this section, we provide several numerical examples. We first show the results for the performance metrics $p(r)$ and $\overline{M}(\rho)$ and evaluate our approximation in Sections IV. We then discuss our broadcast rate optimization method.

The interval of vehicles l_v was fixed to 6 [m] and $\alpha = 4$ in all examples. By considering realistic settings, we chose $\rho_0 = 0.1$ and $T = 15$ [dB]. In addition, $\lambda \triangleq \lambda_x = \lambda_y = 35$ [km^{-1}] and $n_+ = n_- = N$. In each round of the numerical simulation, we first set vehicles in S_Qs and those in S_Rs on the basis of PPPs on roads 10 km long. We then calculated the SIR of each receiver by randomly sampling the value of fading.

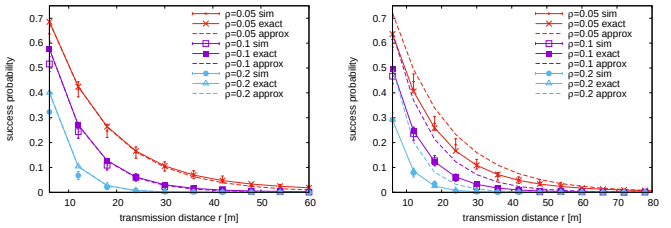

Fig. 3. Comparison of values of $p(r)$ in case (A) from simulation/exact/approximate analysis with different ρ when $N = 25$ and receiver is i-th vehicle from intersection in S_Q (left) and S_{R_y} (right). Each point with error bar (sim), solid line (exact), and dashed line (approx) represent simulation results, our exact model results, and our approximation results.

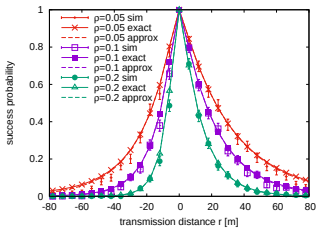

Fig. 4. Comparison of values of $p(r)$ in case (B) from simulation/exact/approximate analysis with different ρ when $N = 25$.

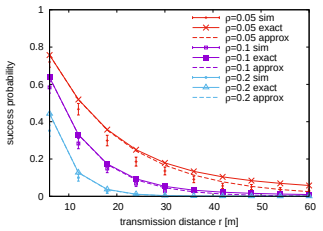

Fig. 5. Comparison of values of $p(r)$ in case (C) from simulation/exact/approximate analysis with different ρ when $N = 25$.

We conducted 10,000 numerical simulations for each graph. Moreover, all error-bars in the graphs in this paper represent 95% confidence intervals.

A. Evaluation of Performance Metrics

We first provide the numerical results for the performance metrics $p(r)$ and $\overline{M}(\rho)$ and evaluate the accuracy of our approximate formulae for them. Figure 3 compares the simulation results and the exact and approximate values of $p(r)$ in case (A), i.e., the case where the transmitter is at the intersection. We calculated the values from exact analysis using (5) and those from approximate analysis using (7) [left graph] and (12) [right graph]. We can see from the left graph that if ρ increases, $p(r)$ also decreases due to higher interference from vehicles in S_Q. We can also see that our approximate formulae fitted well to the results from simulation and exact analysis in all cases and the error became larger when i was larger. Since we assume that N is sufficiently large in our approximation, if the distance from the receiver to the end of the queue is closer, then the approximation error becomes large. From the right graph, we can find that the approximate formulae took higher values than the theoretical results and the error increased subject to ρ. The reason for this is that we approximate the Euclidean distance from the receiver in S_{R_y} to the transmitter at the intersection by the Manhattan distance (see (22) in Appendix). Since the Manhattan distance is larger than the Euclidean distance, the interference became smaller and $p(r)$ became larger than in the simulation and exact analysis. Similarly, Figs. 4 and 5 show the same results in cases (B) and (C). The horizontal axis in Fig. 4 represents the distance to the receiver where the positive (resp. negative) part corresponds to the vehicles in the right-hand (resp. the left-hand) side. The figures show that our approximate formulae achieved quite small errors in all cases. In addition, we can see from Fig. 4 that if ρ is smaller, the results on the positive and negative parts become closer because the interference from the S_Q decreases.

We next show the results for $\overline{M}(\rho)$. Figure 6 compares the simulation results and the exact and approximate values of $\overline{M}(\rho)$. The left, middle, and right graphs correspond to cases (A), (B), and (C), respectively. We can see from the graphs that $\overline{M}(\rho)$ rapidly decreased as ρ increased. In addition, when N was larger, $\overline{M}(\rho)$ became smaller because the interference at the intersection became higher. We can also see that our approximation performed well except for region where $\rho > 0.8$ in case (A). Furthermore, the errors increased when N was small. Similar to the evaluation of $p(r)$, this is because we assume that the queue length N is sufficiently large.

B. Effectiveness of Optimization Method

We next provide the evaluation results for the broadcast rate optimization method. Figure 7 shows the results for the objective function $D(\rho)$ with different ρ and N. We also plotted the optimal ρ_*'s that maximized the approximate $D(\rho)$ in the same graphs. We first focus on the results from the exact analysis. We can see from the graphs that there are local maximum values in the domain $\rho \leq 0.5$ in all cases. The figure shows that the optimal ρ's achieved roughly 1.5 times higher $D(\rho)$ at the maximum than those when $\rho = 0.5$ (unnecessarily high case). We can see a similar tendency in all cases, however, the right graph shows that $D(\rho)$ in case (C) decreased more significantly than the other cases as ρ increased. Recall that neighbors of the transmitter in case (C) exist in S_{R_x} and S_Q while those in case (A) exist in S_{Rx}, S_{R_y}, and S_Q and those in case (B) exist in S_{R_x} and S_Q of only the left part of the transmitter. Thus, if ρ increases, the interference in case (C) becomes higher than (B) and the number of potential receivers (i.e., vehicles not transmitting) in case (C) becomes less than in case (A). This is why our broadcast rate optimization has more significant effect in case (C) than cases (A) and (B). Furthermore, when ρ approached 1, $D(\rho)$ slightly increased. This is because we fixed ρ_0 of the vehicles in S_R. Thus, if ρ increases, the transmitter has more of a chance to transmit to vehicles in S_R even though $p(r)$ becomes smaller. However, $\rho > 0.5$ is unrealistic when considering a receiving time or other computational time. Thus, we consider $\rho_* < 0.5$.

We next discuss the accuracy of our approximation. We can see from the graphs that the approximated values of $D(\rho)$ fit well to those from the exact analysis in the domain $\rho \leq 0.5$. We can also see that the value of ρ_* was not very sensitive to the value of N in all cases. This suggests that our approximate $D(\rho)$ not depending on N is valid. However, the errors became larger due to the assumptions that N is sufficiently large and $(1 - \rho)T > 1$. Fortunately, the errors are relatively small in the domain where ρ_* existed and $\rho \leq 0.5$. Therefore, we can say that the optimization with our approximation provides a good guideline for the optimal ρ_*.

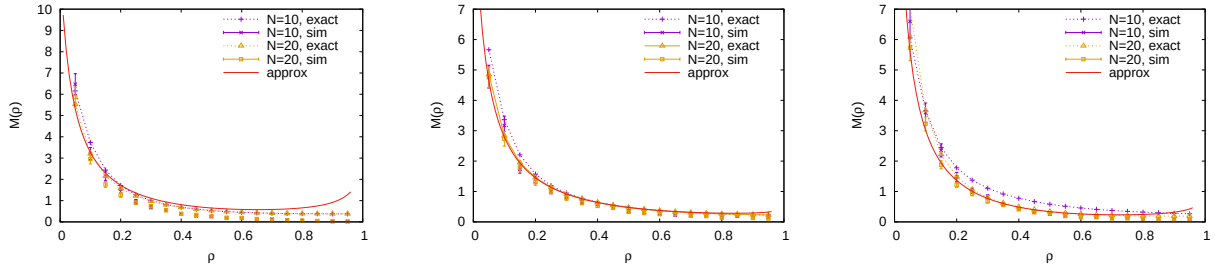

Fig. 6. Comparison of values of $\overline{M}(\rho)$ from simulation/exact/approximate analysis with different ρ and N. Left, middle, and right figures correspond to cases (A), (B), and (C).

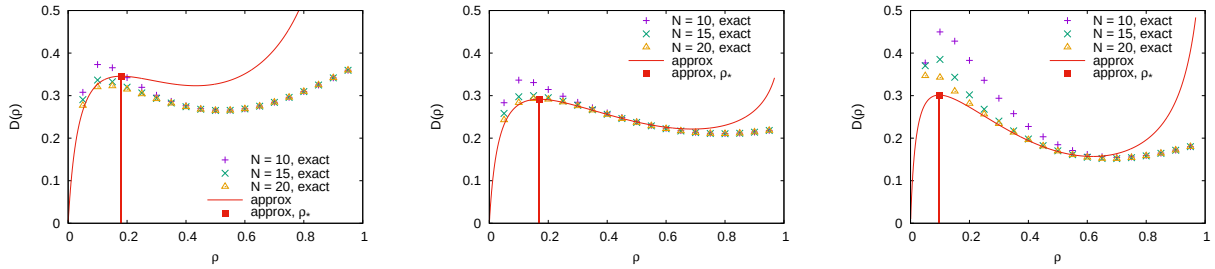

Fig. 7. Comparison of values of $D(\rho)$ from exact/approximate analysis with different ρ and N. Left, middle, and right graphs correspond to cases (A), (B), and (C). Vertical line represents ρ_* that maximizes approximate $D(\rho)$.

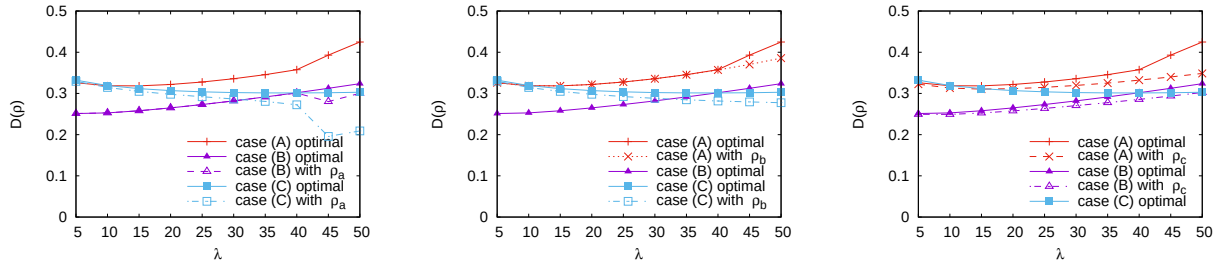

Fig. 8. Comparison of $D(\rho_a)$ (left), $D(\rho_b)$ (middle), and $D(\rho_c)$ (right) in cases (A)–(C) with different λ, where ρ_a, ρ_b, and ρ_c are ρ_* in cases (A)–(C), respectively (dashed lines). Solid lines represent approximate $D(\rho_*)$ in cases (A)–(C).

We now discuss relationship between ρ_*'s in cases (A)–(C). As we mentioned in Section V, our optimization problem depends on the position of a transmitter. Figure 8 compares results of the values of $D(\rho_a)$, $D(\rho_b)$, and $D(\rho_c)$ in cases (A)–(C) with different λ and $N = 25$, where ρ_a, ρ_b and ρ_c are equal to ρ_* in cases (A)–(C), respectively. We also plotted $D(\rho_*)$ in all three cases (A)–(C). We can see from the figure that $D(\rho_*)$ and $D(\rho_a)$, $D(\rho_b)$, and $D(\rho_c)$ in cases (A)–(C) took similar values when λ was smaller than 45. This fact suggests that ρ_* is almost insensitive to cases (A)–(C) if λ is not very high. Thus by adopting a $\rho \in \{\rho_a, \rho_b, \rho_c\}$ to determine the broadcast rate of all vehicles in S_Q, we can roughly maximize $D(\rho)$ regardless of the transmitter position. The reason why the difference between $D(\rho_a)$ and the optimal $D(\rho_*)$ in case (C) [left graph] and that between $D(\rho_c)$ and the optimal $D(\rho_*)$ in case (A) [right graph] increased as λ increased is that if λ is higher, the impacts of interferes and receivers in S_{R_Y} becomes larger and thus the difference between ρ_a and ρ_c becomes larger.

We also evaluate the impact of λ on ρ_*. Figure 9 shows the results for $D(\rho)$ of approximate and exact analysis in case (C) when varying λ. From the figure, we can see that ρ_* increased subject to λ. Recall here that λ is the key parameter for determining the optimal ρ (see Section V). As a result, the results in Figures 8 and 9 show that we can determine the optimal broadcast rate of the vehicles in S_Q by only observing the traffic intensity λ because it is almost insensitive to cases (A)–(C) and the queue length.

C. Vehicles at Other Locations

We next consider the case where a transmitter is at other locations than cases (A)–(C). Since our approximation assumes that N is sufficiently large and only considers special cases (A)–(C), we cannot obtain closed-form formulae for $p(r)$ or $\overline{M}(\rho)$ in general cases. Thus, we aim to roughly estimate their performance by interpolating the values of approximate formulae for cases (A)–(C). Figure 10 shows the values of $p(il_v)$ when varying the positions of the transmitter and the distance to the receiver i in S_Q. We fixed $N = 30$ and $\rho = 0.1$, and the y-axis was in log scale. In the graph, the dashed lines represent the interpolation line using the approximation formulae for cases (A)–(C). From the figure, we can see that

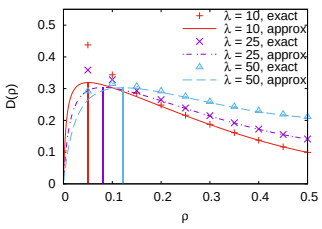

Fig. 9. Comparison of $D(\rho)$ from exact/approximate analysis with different ρ and λ in case (C). Vertical line represents ρ_* that maximizes approximate $D(\rho)$.

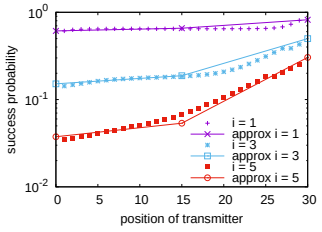

Fig. 10. Comparison of $p(il_v)$ with different position of transmitter from intersection. Dashed line was plotted by interpolating approximate formulae for cases (A)–(C).

the interpolation can roughly estimate the values of $p(il_v)$ in all cases. We can also see that when i increased, the results from the exact analysis became close to log-linear, whereas when i was small, they tended to be a constant value. This is because if the receiver is closer to the transmitter, the impacts of the intersection or the end of the queue rapidly disappear as the distance from the transmitter to them increases.

VII. Conclusion

In this paper, we proposed an optimization method for the broadcast rate in vehicle-to-vehicle (V2V) communications at an intersection based on theoretical analysis. Since the theoretical values of the performance metrics are non-analytical, we provided closed-form approximations for them. By using the closed-form formulae, we can optimize broadcast rate without time-consuming numerical computation. Through numerical examples, we found that our broadcast rate optimization achieved roughly 1.5 times higher performance than the case without broadcast rate control.

In our optimization method, we assume that the traffic intensities in running segments are given. However, vehicles/road side units need to infer these values in a practical situation, e.g., by measuring the distance to the vehicle running at the front. Such inference schemes and their impacts on our optimization method are for future work.

Appendix A
Derivation of Equations (7)–(12)

In this appendix, we explain the derivation of the approximate formulae presented in Section IV-A. For later use, we first introduce an approximate formula for $q_{n_0,T}(r \mid n_1)$ defined as

$$q_{n_0,T}(r \mid n_1) = \sum_{m=1}^{n_1} \log\left(1 + T\left(\frac{r}{n_0+m}\right)^{\alpha}\right). \tag{15}$$

for $n_0, n_1 \in \mathbb{N}$ and $r \in \mathbb{R}_+$. If $T^{-\frac{1}{\alpha}}(n_0+1) \le r < T^{-\frac{1}{\alpha}}(n_0+n_1)$, $q_{n_0,T}(r \mid n_1)$ can be approximated as:

$$\begin{aligned} q_{n_0,T}(r \mid n_1) &\approx (\alpha + \kappa_{1,\alpha} - \kappa_{2,\alpha}) T^{\frac{1}{\alpha}} r - \alpha\left(n_0 + \frac{1}{2}\right)\log T^{\frac{1}{\alpha}} r \\ &- \frac{Tr^{\alpha}}{(\alpha-1)(n_0+n_1)^{\alpha-1}} - \frac{1}{2}\log\left(1 + T\left(\frac{r}{n_0+n_1}\right)^{\alpha}\right) \\ &- \underline{\psi}_{n_0,T}(r) - \frac{1}{2}\log\left(1 + \frac{1}{T}\left(\frac{n_0}{r}\right)^{\alpha}\right) + \kappa_{1,\alpha} + \alpha\log\frac{n_0!}{\sqrt{2\pi}} + \log 2, \end{aligned} \tag{16}$$

where

$$\underline{\psi}_{n_0,T}(r) = n_0 \sum_{k=1}^{\infty} \frac{(-1)^{k+1}}{k(\alpha k+1)T^k}\left(\frac{n_0}{r}\right)^{\alpha k}. \tag{17}$$

The derivation of the above formula is given in [21].

By using the above formula, we first derive (7). To proceed, we temporarily assume that $n_+ = n_- = N$. This assumption will be removed later by considering a sufficiently large N. Since a receiver is at i-th vehicle from the intersection, by substituting $s = T(il_v)^{\alpha}$ into (2), we have

$$\begin{aligned} \mathcal{L}_{I_Q}(T(il_v)^{\alpha} \mid il_v) &= \prod_{m=-n_1, m\neq i,0}^{n_+} \left[\frac{|i-m|^{\alpha}\rho}{|i-m|^{\alpha}+Ti^{\alpha}} + 1 - \rho\right] \\ &= K(\rho) \prod_{m=1}^{N-i} \frac{1 + (1-\rho)T\left(\frac{i}{m}\right)^{\alpha}}{1 + T\left(\frac{i}{m}\right)^{\alpha}} \prod_{m=1}^{N+i} \frac{1 + (1-\rho)T\left(\frac{i}{m}\right)^{\alpha}}{1 + T\left(\frac{i}{m}\right)^{\alpha}}, \end{aligned}$$

where $K(\rho)$ is given in (9). It thus follows from (15) that

$$\begin{aligned} &\log \mathcal{L}_{I_Q}(T(il_v)^{\alpha} \mid il_v) = \log K(\rho) + q_{0,(1-\rho)T}(i \mid N+i) \\ &+ q_{0,(1-\rho)T}(i \mid N-i) - q_{0,T}(i \mid N+i) - q_{0,T}(i \mid N-i). \end{aligned}$$

We now assume that N is sufficiently large. Recall here that $(1-\rho)T \ge 1$ and thus $((1-\rho)T)^{-\frac{1}{\alpha}} < 1$. Therefore, we can apply (16) and thus obtain

$$q_{0,(1-\rho)T}(i \mid \infty) - q_{0,T}(i \mid \infty) \approx \xi_{\alpha,T}(\rho) i - \frac{1}{2}\log(1-\rho),$$

where $\xi_{\alpha,T}(\rho)$ is defined in (8). Combining the above yields

$$\log \mathcal{L}_{I_Q}(T(il_v)^{\alpha} \mid il_v) \approx \log\frac{K(\rho)}{1-\rho} + 2\xi_{\alpha,T}(\rho) i. \tag{18}$$

In addition, from (3) and (4), we can easily obtain

$$\log \mathcal{L}_{I_R^X}(T(il_v)^{\alpha}) = -\rho\lambda_x C^X_{\alpha,T} il_v, \tag{19}$$

$$\log \mathcal{L}_{I_R^Y}(T(il_v)^{\alpha} \mid il_v) = -\rho_0\lambda_y C^Y_{\alpha,T} il_v, \tag{20}$$

where $C^X_{\alpha,T}$ and $C^Y_{\alpha,T}$ are given in (10). As a result, combining (18)–(20) with (5) yields (7).

We now move on to the derivation of (11). To proceed, we temporarily assume that $r = r_0 l_v$ ($r_0 \in \mathbb{N}$). By following the same arguments in the derivation of (18), we have

$$\begin{aligned} \log \mathcal{L}_{I_Q}(Tr^{\alpha} \mid r) &= \sum_{m=-n_1, m\neq 0}^{n_+} \log\left[\frac{|r_0-m|^{\alpha}\rho}{|r_0-m|^{\alpha}+Ti^{\alpha}} + 1 - \rho\right] \\ &= \log(1-\rho) + q_{0,(1-\rho)T}(r_0 \mid N+r_0) + q_{0,(1-\rho)T}(r_0 \mid N-r_0) \\ &\quad - q_{0,T}(r_0 \mid N+r_0) - q_{0,T}(r_0 \mid N-r_0) + \log K(\rho) \\ &\approx 2\xi_{\alpha,T}(\rho)\frac{r}{l_v} + \log K(\rho), \end{aligned} \tag{21}$$

where the last approximation follows from (16), $N \to \infty$ and $r_0 := r/l_v \in \mathbb{R}$. From this, (19), and (20), we obtain (11).

Finally, we derive (12). Since the receiver is in S_{R_y} at distance r from the intersection, its Euclidean distance from the i-th vehicle from the intersection is equal to $\sqrt{r^2 + (il_v)^2}$. However, applying this Euclidean distance to $\mathcal{L}_I(Tr^{\alpha})$ leads to mathematically intractable analysis. Thus, we approximate this by using Manhattan distance, which is equal to $r + il_v$. In other words, the Laplace transform of I_Q can be approximated as

$$\mathcal{L}_{I_Q}(Tr^{\alpha} \mid r) = \prod_{m=-n_-, m\neq 0}^{n_+} \frac{1 + (1-\rho)T\left(\frac{r_0}{r_0+|m|}\right)^{\alpha}}{1 + T\left(\frac{r_0}{r_0+|m|}\right)^{\alpha}}. \tag{22}$$

By considering sufficiently large n_+ and n_-, we obtain

$$\log \mathcal{L}_{I_Q}(Tr^\alpha \mid r) \approx 2\left(q_{r_0,(1-\rho)T}(r_0 \mid \infty) - q_{r_0,T}(r_0 \mid \infty)\right).$$

Since $((1-\rho)T)^{-\frac{1}{\alpha}} < 1$, we can apply (16) to this and thus obtain

$$\log \mathcal{L}_{I_Q}(Tr^\alpha | r) \approx 2\left[\xi_{\alpha,T}(\rho) - \log(1-\rho) - \frac{\rho}{(\alpha+1)(1-\rho)T}\right] r_0 - \log(1-\rho) + \log\frac{(1-\rho)(1+T)}{1+(1-\rho)T}, \quad (23)$$

where we use the following approximation [see (17)]

$$\underline{\psi}_{r_0,(1-\rho)T}(r_0) - \underline{\psi}_{r_0,T}(r_0) = r_0 \sum_{k=1}^{\infty} \frac{(-1)^{k+1}}{k(\alpha k+1)T^k} = \frac{r_0}{(\alpha+1)T}\frac{\rho}{1-\rho} + O(((1-\rho)T)^2). \quad (24)$$

Although the receiver is on the y-axis, $p(r)$ can be calculated very similarly to Proposition 1. As a result, by using (19)–(23), we have (12).

Appendix B
Approximate Formulas For Case (B)

In this appendix, we give approximate formulae for the performance metrics in case (B). The derivation of these formulae are given in [21].

Approximate formulae of $p(r)$ in case (B): Suppose that the transmitter is at the end of the queue and $(1-\rho)T \geq 1$. If $\alpha \in \mathbb{N}$, the probability of successful transmission can be approximated as follows: (i) If a receiver is in S_Q and the i-th vehicle from the end of the queue, then

$$p(il_v) \approx K(\rho) e^{\frac{\rho}{2(1-\rho)T}} (1-\rho)^{i-\frac{1}{2}} e^{\left(\beta_{\alpha,T}(\rho) - \rho_0 \lambda_x C^X_{\alpha,T} l_v\right) i}$$

where

$$\beta_{\alpha,T}(\rho) = \xi_{\alpha,T}(\rho) + \frac{\rho}{(1-\rho)(\alpha+1)T},$$

(ii) if a receiver is in S_{R_x} in the negative part and at distance $r > 0$ from the end of the queue, then

$$p(r) \approx K(\rho) e^{\frac{\rho}{2(1-\rho)T}} (1-\rho)^{\frac{r}{l_v}+\frac{1}{2}} e^{\left(\frac{\beta_{\alpha,T}(\rho)}{l_v} - \rho_0 \lambda_x C^X_{\alpha,T}\right)},$$

and (iii) if a receiver is in S_{R_x} in the positive part and at distance $r > 0$ from the end of the queue, then

$$p(r) \approx \sqrt{K(\rho)}(1-\rho)^{-\frac{r}{l_v}} \exp\left[\left(\frac{\xi_{\alpha,T}(\rho)}{l_v} - \frac{\rho}{(\alpha+1)(1-\rho)Tl_v} - \rho_0 \lambda_x C^X_{\alpha,T}\right) r\right]. \quad (25)$$

Approximate formulae of $\overline{M}$ in case (B):

$$\overline{M}_Q(\rho) \approx \sqrt{1-\rho}\exp\left(\frac{\rho}{2(1-\rho)T}\right) K(\rho) \times \frac{\exp\left(\beta_{\alpha,T}(\rho) - \rho_0 \lambda_x C^X_{\alpha,T} l_v\right)}{1-(1-\rho)\exp\left(\beta_{\alpha,T}(\rho) - \rho_0 \lambda_x C^X_{\alpha,T} l_v\right)}, \quad (26)$$

$$\overline{M}_{R_X}(\rho) \approx \sqrt{1-\rho}\exp\left(\frac{\rho}{2(1-\rho)T}\right) K(\rho) \times \frac{(1-\rho_0)\lambda_x l_v}{\beta_{\alpha,T}(\rho) + \log(1-\rho) - \rho_0 \lambda_x C^X_{\alpha,T} l_v} + (1-\rho_0)\lambda_x l_v \sqrt{K(\rho)} \times \left[\xi_{\alpha,T}(\rho) - \log(1-\rho) - \frac{\rho}{(\alpha+1)(1-\rho)T} - \rho_0 \lambda_x C^X_{\alpha,T} l_v\right]^{-1}.$$

References

[1] H. Hartenstein and K. Laberteaux, *VANET Vehicular Applications and Inter-Networking Technologies*. New York: Wiley, 2009.

[2] *Wireless Access in Vehicular Environment (WAVE) in Standard 802.11, Specific Requirements,* IEEE Std. 802.11p/D1.0, Feb. 2006.

[3] Vehicle Safety Commun. Consortium (VSCC), Vehicle safety communications project, task 3 final report: Identify intelligent vehicle safety applications enabled by DSRC, Nat. Highway Traffic Safety Admin., Washington DC, USA, 2005.

[4] C.-L. Huang, Y. P. Fallah, R. Sengupta, and H. Krishnan, "Adaptive intervehicle communication control for cooperative safety systems," *IEEE Network*, vol. 24, no. 1, pp. 6–13, 2010.

[5] Y. P. Fallah, C. Huang, R. Sengupta, and H. Krishnan, "Congestion control based on channel occupancy in vehicular broadcast networks," In *Proc. VTC-2010 Fall* 2010.

[6] Y. P. Fallah, N. Nasiriani, and H. Krishnan, "Stable and fair power control in vehicle safety networks," *IEEE Trans. on Veh. Technol.*, vol. 65, no. 3, pp. 1662–1675, 2016.

[7] T. Tielert, D. Jiang, Q. Chen, L. Delgrossi, and H. Hartenstein, "Design methodology and evaluation of rate adaptation based congestion control for vehicle safety communications," In *Proc. VNC*, 2011.

[8] M. T.-Moreno, J. Mittag, P. Santi, and H. Hartenstein, "Vehicle-to-vehicle communication: fair transmit power control for safety-critical information," *IEEE Trans. on Veh. Technol.*, vol. 58, no. 7, pp. 3684–3703, 2009.

[9] J. Mittag, F. Schmidt-Eisenlohr, M. Killat, J. Härri, and H. Hartenstein, "Analysis and design of effective and low-overhead transmission power control for VANETs," In *Proc. VANET*, 2008, pp.39–48.

[10] B. Błaszczyszyn, P. Muhlethaler, and Y. Toor, "Stochastic analysis of Aloha in vehicular ad-hoc networks," *Ann. Telecommun.*, vol. 68, no. 1, pp. 95–106, 2012.

[11] M. J. Farooq, H. ElSawy, and M.-S. Alouini, "Modeling inter-vehicle communication in multi-lane highways: a stochastic geometry approach," In Proc. VTC-2015 Fall, 2015.

[12] T. V. Nguyen, F. Baccelli, K. Zhu, S. Subramanian, and W. Wu, "A performance analysis of CSMA based broadcast protocol in VANETs," In *Proc. INFOCOM*, 2013.

[13] Z. Tong, H. Lu, M. Haenggi, and C. Poellabauer, "A stochastic geometry approach to the modeling of DSRC for vehicular safety communication," *IEEE Trans. on Intell. Transp. Syst.*, vol. 17, no. 5, pp. 1448–1458, 2016.

[14] T. V. Nguyen, F. Baccelli, and D. Kofman, "A stochastic geometry analysis of dense IEEE 802.11 networks," In *Proc. INFOCOM*, 2007.

[15] V. V. Chetlur and H. S. Dhillon, "Coverage analysis of a vehicular network modeled as Cox process driven by Poisson line process," *IEEE Trans. on Wireless Commun.*, vol. 17, no. 7, pp. 4401–4416, 2018.

[16] C. Choi and F. Baccelli, "An analytical framework for coverage in cellular networks leveraging vehicles," *IEEE Trans. on Commun.*, vol. 66, no. 10, pp. 4950–4964, 2018.

[17] E. Steinmetz, M. Wildemeersch, T. Q. S. Quek, and H. Wymeersch, "A stochastic geometry model for vehicular communication near intersections," In *Proc. GLOBECOM'15*, 2015.

[18] T. Kimura and H. Saito, "Theoretical interference analysis of inter-vehicular communication at intersection with power control," *Comput. Commun.,* vol. 117, pp. 84–103, 2018.

[19] G. Karagiannis, O. Altintas, E. Ekici, G. Heijenk, B. Jarupan, K. Lin, and T. Wei, "Vehicular networking: a survey and tutorial on requirements, architectures, challenges, standards and solutions," *IEEE Commun. Surveys Tuts.*, vol. 13, no. 4, pp. 584–616, 2011.

[20] H. ElSawy and E. Hossain, "A modified hard core point process for analysis of random CSMA wireless networks in general fading environments," *IEEE Trans. Commun.*, vol. 61, no. 4, pp. 1520–1534, 2013.

[21] T. Kimura and H. Saito, "Theoretical performance analysis of vehicular broadcast communications at intersection and their optimization," arXiv:1706.09606 (available at https://arxiv.org/abs/1706.09606).

[22] F. Baccelli and B. Błaszczyszyn, *Stochastic Geometry and Wireless Networks, Volume I -Theory.* Now Publishers, Hanover, 2009.